

From G_2 to $SO(8)$: Emergence and reminiscence of supersymmetry and triality

Zhi-Qiang Gao^a and Congjun Wu^{b,c,d,e,1}

^a*Department of Physics, University of California, Berkeley, California 94720, USA*

^b*New Cornerstone Science Laboratory, Department of Physics, School of Science, Westlake University, Hangzhou 310024, Zhejiang, China*

^c*Institute for Theoretical Sciences, Westlake University, Hangzhou 310024, Zhejiang, China*

^d*Key Laboratory for Quantum Materials of Zhejiang Province, School of Science, Westlake University, Hangzhou 310024, Zhejiang, China*

^e*Institute of Natural Sciences, Westlake Institute for Advanced Study, Hangzhou 310024, Zhejiang, China*

E-mail: zqgao@berkeley.edu, wucongjun@westlake.edu.cn

ABSTRACT: We construct a (1+1)-dimension continuum model of 4-component fermions incorporating the exceptional Lie group symmetry G_2 . Four gapped and five gapless phases are identified via the one-loop renormalization group analysis. The gapped phases are controlled by four different stable $SO(8)$ Gross-Neveu fixed points, among which three exhibit an emergent triality, while the rest one possesses the self-triality, i.e., invariant under the triality mapping. The gapless phases include three $SO(7)$ critical ones, a G_2 critical one, and a Luttinger liquid. Three $SO(7)$ critical phases correspond to different $SO(7)$ Gross-Neveu fixed points connected by the triality relation similar to the gapped $SO(8)$ case. The G_2 critical phase is controlled by an unstable fixed point described by a direct product of the Ising and tricritical Ising conformal field theories with the central charges $c = \frac{1}{2}$ and $c = \frac{7}{10}$, respectively, while the latter one is known to possess spacetime supersymmetry. In the lattice realization with a Hubbard-type interaction, the triality is broken into the duality between two $SO(7)$ symmetries and the supersymmetric G_2 critical phase exhibits the degeneracy between bosonic and fermionic states, which are reminiscences of the continuum model.

¹Corresponding author.

Contents

1	Introduction	1
2	The model Hamiltonians	2
2.1	The minimal G_2 symmetric lattice model	2
2.2	The coarse-grained continuum model in (1+1)D	4
3	Renormalization group flows and fixed planes	5
3.1	The $SO(7)$ symmetric fixed planes	5
3.2	The G_2 critical fixed planes	7
3.3	Phase diagrams in fixed bodies	9
4	Embedding of the lattice model	10
5	Conclusions	13
A	Fermion bilinears and majorana operators in the lattice model	16
B	RG equations	18
C	Bosonization of the interaction on $SO(7)$ symmetric fixed planes	22
D	RG for the lattice model	23

1 Introduction

Exceptional Lie groups play an essential role in the study of modern condensed matter physics [1–4]. E_8 , the largest exceptional Lie group, is employed to describe an exotic quantum Hall state [5]. The E_8 excitations are also observed in an anti-ferromagnetic Ising spin chain [2]. On the other hand, the smallest exceptional Lie group G_2 with rank-2 and 14 dimensional [6], which is the automorphism group of the non-associative algebra octonion [7], has especially attracted many interests recently [8–11]. In particular, a lattice model which has an explicit G_2 symmetry based on 4-component, such as spin- $\frac{3}{2}$, fermions is constructed [9]. However, G_2 symmetry is shown to be intrinsically strongly correlated, that it cannot be realized in non-interacting systems [9], which makes it hard to study analytically.

Inspired by Ref. [12], we investigate the coarse-grained version of the lattice G_2 model [9] in (1+1) spacetime dimension, where many powerful tools can be utilized to study strong correlation systems. Through an one-loop renormalization group (RG) calculation, we reveal the hidden $SO(8)$ triality structure. The phase diagram is consistent with the

mean-field analysis in the lattice model [9]. Interestingly, we also find in the phase diagram that one critical phase is described by the tricritical Ising (TCI) conformal field theory (CFT) [13]. TCI CFT actually has spacetime supersymmetry [14, 15], which is corresponding to the degeneracy between bosonic and fermionic states in the lattice model [9]. Coset constructions based on G_2 Wess-Zumino-Witten (WZW) models realizing exotic non-Abelian statistics [8, 10, 11] can also emerge in our model. Moreover, our model also exhibits the exotic phenomena of multiversality and unnecessary criticality [16, 17].

The rest part of this article is organized as follows: In Section 2, the models are introduced both in the form of the lattice Hamiltonian and in the coarse-grained continuum version. In Section 3, the one-loop RG analyses are performed to yield the RG flow patterns and the corresponding gapped and critical phases. The embedding of the lattice model in the phase diagram of the continuum model is presented in Section 4. Conclusions are presented in Section 5.

2 The model Hamiltonians

2.1 The minimal G_2 symmetric lattice model

In a preceding work [9], we construct a minimal lattice model with the G_2 symmetry based on 4-component spin- $\frac{3}{2}$ fermions as briefly reviewed below. The 4-component spinor $\psi_\sigma(i)$ defined on each site i with $\sigma = \pm\frac{3}{2}, \pm\frac{1}{2}$ spans a local $SO(8)$ algebra $\{N_{ab}(i)\}$ with $0 \leq a, b \leq 7$ [9, 18, 19]. Here each generator $N_{ab}(i)$ is a fermion bilinear operator in the particle-hole or particle-particle channel.

An $SO(5)$, or, isomorphically, $Sp(4)$ subalgebra of $SO(8)$ is simply $L_{ab} = N_{ab} = \frac{1}{2}\psi^\dagger(i)\Gamma_{ab}\psi(i)$ with $1 \leq a, b \leq 5$, where Γ_{ab} 's are the commutators among the five rank-2 anti-commuting Γ -matrices, i.e., $\Gamma_{ab} = \frac{i}{2}[\Gamma_a, \Gamma_b]$ with $\{\Gamma_a, \Gamma_b\} = 2\delta_{ab}$. The 10 generators of $Sp(4)$ unify both spin and spin-octupole operators based on the spin- $\frac{3}{2}$ spinor ψ . An $SO(7)$ subalgebra, denoted as $SO(7)_A$ below, is an extension of $Sp(4)$, defined as $M_{ab}(i) = N_{ab}(i)$ with $0 \leq a, b \leq 6$. It further includes, and hence, unifies the particle number $M_{06}(i) = \frac{1}{2}(\psi^\dagger(i)\psi(i) - 2)$, and the pairing operators in the spin quintet channel $M_{0a}(i) = \frac{1}{2}\psi^\dagger(i)\Gamma_a R\psi^\dagger(i)$ with $1 \leq a \leq 5$ where R is the charge conjugation matrix satisfying $R^T = R^{-1} = -R$. Pairing operators are complex, and one complex operator is equivalent to two real ones. The rest 7 operators denoted $V_a(i) = N_{a7}(i)$ form a vector representation of the $SO(7)_A$ defined above, unifying 5 spin quadrupole operators with $N_{a7} = \frac{1}{2}\psi^\dagger(i)\Gamma^a\psi(i)$ with $1 \leq a \leq 5$ and 1 complex singlet pairing operator $N_{07} = \psi^\dagger(i)R\psi^\dagger(i)$. For details please refer to appendix A.

The $SO(7)_A$ algebra defined above can be decomposed into a 14-dimensional G_{ab} part spanning the G_2 subalgebra and a 7-vector T_a belonging to the coset $SO(7)_A/G_2$ defined as [9]

$$G_{ab}(i) = \frac{2}{3}M_{ab}(i) + \frac{1}{6}C_{abcd}M_{cd}(i), \quad T_a(i) = \frac{1}{2\sqrt{3}}C_{abc}M_{bc}(i), \quad (2.1)$$

where C_{abcd} is the structure constant of the non-associative octonion algebra. Note that $G_{ab}(i)$ satisfy 7 constraints $C_{abc}G_{ab}(i) = 0$, where $C_{abc} = \frac{1}{24}\epsilon_{abcdefg}C_{defg}$ is the dual tensor

of C_{abcd} . Therefore, only 14 of them are linear independent. $T_a(i)$ transform under the vector representation of G_2 [9, 20]. $V_a(i)$ defined before also form a G_2 vector representation [9, 20]. Inversely, the $SO(7)_A$ generators can be represented by $G_{ab}(i)$ and $T_a(i)$ as

$$M_{ab}(i) = G_{ab}(i) + \frac{1}{\sqrt{3}}C_{abc}T_c(i). \quad (2.2)$$

Another $SO(7)$ algebra denoted as $SO(7)_B$ is constructed below sharing the same G_2 subalgebra as in $SO(7)_A$. Define operators $T'_a(i)$ and $V'_a(i)$ as a “120° rotation” of $T_a(i)$ and $V_a(i)$:

$$T'_a(i) + iV'_a(i) = e^{i\frac{2}{3}\pi}(T_a(i) + iV_a(i)). \quad (2.3)$$

The generators of $SO(7)_B$ are expressed as [9],

$$M'_{ab}(i) = G_{ab}(i) + \frac{1}{\sqrt{3}}C_{abc}T'_c(i), \quad (2.4)$$

and $V'_a(i)$ form an vector representation of $SO(7)_B$. The Casimirs of these two $SO(7)$'s are connected by the duality relations [9],

$$\begin{aligned} C_A(i) &= \sum_{0 \leq a < b \leq 6} M_{ab}(i)M_{ab}(i) = \frac{1}{4} \sum_{abcd} C_{abcd}M'_{ab}(i)M'_{cd}(i), \\ C_B(i) &= \sum_{0 \leq a < b \leq 6} M'_{ab}(i)M'_{ab}(i) = \frac{1}{4} \sum_{abcd} C_{abcd}M_{ab}(i)M_{cd}(i). \end{aligned} \quad (2.5)$$

A lattice model $H = H_0 + H_{int}^{G_2}$ realizing the G_2 symmetry has been constructed as the intersection between $SO(7)_A$ and $SO(7)_B$ symmetries [9],

$$\begin{aligned} H_0 &= -t_{\text{hop}} \sum_{\langle ij \rangle, \sigma} \left(\psi_\sigma^\dagger(i) \psi_\sigma(j) + h.c. \right), \\ H_{\text{int}}^{G_2} &= u \sum_i C_A(i) + v \sum_i C_B(i), \end{aligned} \quad (2.6)$$

where u and v are coupling constants. When $v = 0$, or, $u = 0$, the lattice model of (2.6) restores the $SO(7)_A$, or, $SO(7)_B$ symmetry, respectively.

Besides the $SO(7)_A$ and $SO(7)_B$ symmetries in the lattice model of (2.6), there exists a third $SO(7)_M$ one sharing the same G_2 sub-group, where M stands for Majorana. Its generators $M''_{ab}(i)$ can be similarly defined through (2.4), with $T'_a(i)$ and V'_a substituted by $T''_a(i)$ and V''_a defined by “-120° rotation”, i.e., $T''_a(i) + iV''_a(i) = e^{-i\frac{2}{3}\pi}(T_a(i) + iV_a(i))$. The $SO(7)_M$ algebra can be naturally expressed in terms of Majorana fermions constructed based on the 4-component spinor $\psi_\sigma(i)$, i.e., $\chi_m(i)$ with $0 \leq m \leq 7$ (see appendix A for a detailed definition). By straightforward calculations, we express M''_{ab} and $V''_a(i)$ as

$$M''_{ab}(i) = i\chi_m(i)\chi_n(i), \quad V''_a(i) = i\chi_0(i)\chi_m(i), \quad (2.7)$$

where $1 \leq m \leq 7$. As $(i\chi_m(i)\chi_n(i))^2$ is always equal to 1, the Casimir of $SO(7)_M$ is a c -number. Therefore, it is absent in the lattice Hamiltonian (2.6) where the on-site Hubbard-type interactions are written in terms of Casimirs. Nevertheless, in the coarse-grained continuum model, the $SO(7)_M$ symmetry will emerge at low energy and fulfill the $SO(8)$ triality relation.

2.2 The coarse-grained continuum model in (1+1)D

In (1+1)D, the low energy effective theory of the free Hamiltonian H_0 in (2.6) is the $SO(8)_1$ WZW model [21] expressed in terms of Majorana fields $\chi_m^{R/L}$ with $0 \leq m \leq 7$. These Majorana fields $\chi_m(i)$ defined above form the 8-dimensional vector representation of the $SO(8)$ symmetry. The disorder operators of the $SO(8)_1$ WZW model build another two sets of Majorana fermions spanning the 8-dimensional spinor and anti-spinor representations [21]. Hence, when the $SO(8)$ symmetry is broken to $SO(7)$, three different choices are possible such that one of the three 8-dimensional representations is decomposed to $8 = 7 \oplus 1$ under the $SO(7)$ while the other two remain 8-dimensional. If this residual $SO(7)$ symmetry is chosen to be $SO(7)_M$, then χ_0 is the singlet invariant under $SO(7)_M$, and $\chi_{1,2,\dots,7}$ form the 7-dimensional vector of $SO(7)_M$. The triality relation among the three 8-dimensional $SO(8)$ representations is inherited by that among $SO(7)$ symmetries.

The chiral currents $G_{ab}^{R/L}$, $T_a^{R/L}$, and $V_a^{R/L}$ in the coarse-grained model are defined as fermion bilinears similar to their lattice cousins, with $\psi_\sigma(i)$ substituted by $\psi_{R,\sigma}(z)$ and $\psi_{L,\sigma}(\bar{z})$ for the right- and left-moving fermions, respectively. Note that Umklapp terms $\psi_R^\dagger \psi_R^\dagger \psi_L \psi_L$ and $\psi_L^\dagger \psi_L^\dagger \psi_R \psi_R$ (spin indices omitted) are allowed, since H_0 should be at half-filling to maintain the G_2 symmetry. Any linear combination of T_a and V_a form a G_2 vector. Therefore, in terms of $SO(7)_A$ operators, the most general form of the G_2 invariant low energy effective Hamiltonian density reads

$$\mathcal{H}_{\text{int}} = g \sum_{a \neq b} G_{ab}^R G_{ab}^L + t \sum_a T_a^R T_a^L + y \sum_a V_a^R V_a^L + \frac{w}{\sqrt{2}} \sum_a (T_a^R V_a^L + V_a^R T_a^L), \quad (2.8)$$

where g , t , y , and w are coupling constants. The $SO(7)_A$ symmetry appears at $w = 0$, $t = 2g$, and y arbitrary.

To explicitly reveal the triality relation, the Hamiltonian density (2.8) is rewritten in an equivalent way as

$$\mathcal{H}_{\text{int}} = g \sum_{a \neq b} G_{ab}^R G_{ab}^L + t_A \sum_a T_a^R T_a^L + t_B \sum_a T_a'^R T_a'^L + t_M \sum_a T_a''^R T_a''^L, \quad (2.9)$$

with the relation

$$t_A = t - \frac{1}{3}y, \quad t_B = \frac{2}{3}y + \frac{\sqrt{6}}{3}w, \quad t_M = \frac{2}{3}y - \frac{\sqrt{6}}{3}w. \quad (2.10)$$

The triality of the three $SO(7)$ symmetries is already implied in the permutation of three coupling constants t_A , t_B , and t_M .

3 Renormalization group flows and fixed planes

Based on the G_2 current algebra [20], we perform the one-loop RG calculation in appendix B, yielding the following RG equations for the coupling constants defined in (2.8),

$$\begin{aligned}\frac{dg}{dl} &= 16g^2 + t^2 + y^2 + w^2, \\ \frac{dt}{dl} &= 16gt + 2t^2 + 2y^2 - 2w^2, \\ \frac{dy}{dl} &= 16gy + 4ty + 2w^2, \\ \frac{dw}{dl} &= 16gw - 4tw + 4yw.\end{aligned}\tag{3.1}$$

For illustrating of the triality explicitly, the RG equations (3.1) can be cast in terms of g and t_i with $i \in \{A, B, M\}$ in a more symmetric form as

$$\begin{aligned}\frac{dg}{dl} &= 16g^2 + \sum_i t_i^2 + \frac{1}{4} \sum_{i \neq j} t_i t_j, \\ \frac{dt_i}{dl} &= 16gt_i + 2t_i^2 + 4 \frac{t_A t_B t_M}{t_i}.\end{aligned}\tag{3.2}$$

An analytical solution to the RG equations (3.2) would be difficult, however, the geometrical structure of the RG flows is rather clear. They exhibit fixed planes (not necessarily the same as critical surfaces) in which the RG flows keep in-plane evolutions. The fixed planes can be classified into two types, the $SO(7)$ symmetric and the G_2 critical, respectively, as discussed below.

3.1 The $SO(7)$ symmetric fixed planes

There exist three planes in which the G_2 symmetry is enlarged to the $SO(7)_A$, $SO(7)_B$, and $SO(7)_M$ symmetries, respectively. They are related to each other by the triality relation as well as the RG flow patterns. The RG equations with $SO(7)$ symmetry have been investigated in literature [22, 23]. For the self-contentedness of this work, we summarize the corresponding stable and critical quantum phases.

For an $SO(7)$ plane, the coupling constants satisfy the following relation,

$$SO(7)_i \text{ symmetric fixed plane } P_i : t_j = t_k = 4g - 2t_i,\tag{3.3}$$

where $\{i, j, k\}$ are permutations of $\{A, B, M\}$. Within these $SO(7)$ fixed planes, the RG equations can be solved analytically. The resulting fixed points (flows) characterize different quantum phases and phase transitions.

Taking the plane of P_A as an example, the $SO(7)_A$ symmetry is explicit as seen from the reduced interaction Hamiltonian density,

$$\mathcal{H}_A = g \sum_{a \neq b} M_{ab}^R M_{ab}^L + y \sum_a V_a^R V_a^L.\tag{3.4}$$

The RG equations in the $SO(7)_A$ symmetric plane P_A are reduced to

$$\frac{dg}{dl} = 20g^2 + y^2, \quad \frac{dy}{dl} = 24gy. \quad (3.5)$$

The solutions to RG equations (3.5) can be classified in the following cases.

Case (I): *The fully gapped $SO(8)$ Gross-Neveu (GN) phases.* There exists a stable $SO(8)$ GN [24] fixed flow characterized by the interaction parameter set of $y = t = 2g \rightarrow +\infty$ and $w = 0$, or, equivalently, $t_A = t_B = t_M = \frac{4}{3}g \rightarrow +\infty$. The Hamiltonian density along this line is reduced to

$$\mathcal{H}_{\text{GN}}^{SO(8)} = g \sum_{a \neq b} M_{ab}^R M_{ab}^L + 2g \sum_a V_a^R V_a^L = g \sum_{a \neq b} N_{ab}^R N_{ab}^L, \quad (3.6)$$

which describes the fully gapped $SO(8)$ GN phase. This fixed flow is at the intersection of three $SO(7)_i$ fixed planes with $i \in \{A, B, M\}$ and is invariant under the permutation of t_i . Therefore, it exhibits $SO(8)$ self-triality.

Another $SO(8)$ phase is also stable characterized by the fixed point of $y = -t = -2g \rightarrow -\infty$ and $w = 0$, or, equivalently, $t_B = t_M = -\frac{1}{2}t_A = -\frac{4}{3}g \rightarrow -\infty$. Along this line, the interaction Hamiltonian density is reduced to

$$\mathcal{H}_{\text{GN}}^{SO(8)_A} = g \sum_{a \neq b} M_{ab}^R M_{ab}^L - 2g \sum_a V_a^R V_a^L. \quad (3.7)$$

It is related to the previous $SO(8)$ phase of (3.6) by the chiral transformation [21, 23] which keeps the current of left-movers but change that of right-movers to $\{M_{ab}^R, -V_a^R\}$. Such a phase is also fully gapped denoted as the $SO(8)_A$ GN phase.

Case (II): *The critical $SO(7)$ GN phase.* This phase is controlled by the unstable $SO(7)$ GN fixed flow characterized by $t = 2g \rightarrow +\infty$ and $y = w = 0$, or, equivalently, $t_B = t_M = 0$, $t_A = 2g \rightarrow +\infty$. Along this flow, the interaction Hamiltonian density is reduced to

$$\mathcal{H}_{\text{GN}}^{SO(7)_A} = g \sum_{a \neq b} M_{ab}^R M_{ab}^L. \quad (3.8)$$

In such a state, 7 Majorana modes are gapped out by the GN-type interaction while 1 Majorana mode remains gapless [23, 25]. It describes a critical phase with the $SO(7)_A$ symmetry, sandwiched by two gapped $SO(8)$ phases discussed previously. This critical phase, denoted as the $SO(7)_A$ GN phase, has the central charge of $c = \frac{1}{2}$ attributed to the gapless Majorana mode, yielding a phase transition in the Ising universality class. The two gapped $SO(8)$ phases are Ising dual to each other.

Case (III): *The critical $SO(8)_1$ WZW phase.* This phase is characterized by the unstable fixed point of $g = t = y = w = 0$, or, equivalently, $g = t_A = t_B = t_M = 0$. Its central charge $c = 4$ corresponding to the free theory of 8 Majoranas, i.e., the $SO(8)_1$ WZW model. It controls the gapless Luttinger liquid phase. Apparently, this fixed point also exhibits self-triality.

Due to the triality, RG flows and the stable phases of the $SO(7)_B$ and $SO(7)_M$ symmetric fixed planes should exhibit the same structure as the case of $SO(7)_A$. Hence, three

$SO(8)_i$ ($i = A, B, M$) gapped phases are related to each other by the triality. The phase transitions between the gapped $SO(8)$ GN phase and $SO(8)_i$ GN phases are in the Ising universality class with central charge $c = \frac{1}{2}$, controlled by $SO(7)_i$ GN fixed flows. The three $SO(7)_i$ GN points, as well as the three critical Ising phases are also related to each other by the triality relation.

The schematic RG flows and the phase diagram on the $SO(7)_A$ symmetric fixed plane P_A are shown in figure 1. By substituting the subscript A by B/M , the similar physics appears on $SO(7)_{B/M}$ symmetric fixed planes. The lattice model (2.6) with $v = 0$ possesses the $SO(7)_A$ symmetry. As varying u , its phase evolution is also marked in figure 1. In appendix C, we provide a standard bosonization analysis [21–23, 26], which gives rise to the same phase diagram.

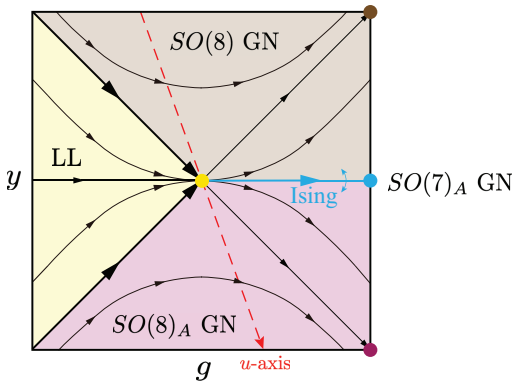


Figure 1. The RG flows and phase diagram on the $SO(7)_A$ symmetric fixed plane. The horizontal and vertical axes are labeled by g and y , respectively. Phase boundaries are marked by thick lines. The $SO(8)$ GN, $SO(8)_A$ GN, and $SO(7)_A$ GN fixed points (defined as $g \rightarrow +\infty$ points of the fixed flows) are marked by brown, blue, and crimson dots, respectively. The yellow dot stands for the free Majorana fixed point. “LL” denotes the Luttinger liquid phase. The transition between the $SO(8)$ GN phase and the $SO(8)_A$ GN phase is described by the critical $SO(7)_A$ GN phase in the Ising universality class. Phase structures in the $SO(7)_{B/M}$ fixed planes can be obtained via the triality mapping. The embedding of the u -axis in the lattice model phase diagram is colored in red.

3.2 The G_2 critical fixed planes

Aside from the GN-type fixed flows discussed above, the RG equations (3.1) have an unstable flow away from all the three $SO(7)$ symmetric fixed planes. This G_2 symmetric fixed flow is characterized by $g \rightarrow +\infty$ and $t = y = w = 0$, or, equivalently, $g \rightarrow +\infty$, $t_A = t_B = t_M = 0$, which exhibits the self-triality. The corresponding interaction Hamiltonian density reads,

$$\mathcal{H}_{\text{TCI}}^{G_2} = g \sum_{a \neq b} G_{ab}^R G_{ab}^L. \quad (3.9)$$

Interestingly, $g \rightarrow +\infty$ does not completely gap out the spectra, but results in a tricritical Ising (TCI) phase [8, 13] with central charge $c = \frac{7}{10}$. The emergent symmetry of this

critical phase is not only G_2 , but also the $\mathcal{N} = 1$ spacetime supersymmetry inherited from the TCI CFT [14, 15].

In the Majorana basis, (3.9) contains only 7 of the 8 Majorana modes, and the decoupled one χ_0 remains gapless. Hence, the total central charge is $c = \frac{7}{10} + \frac{1}{2} = \frac{6}{5}$. A CFT with such a central charge has a parafermion representation [27–29], which may be realized on the edge of certain fractional quantum Hall states [28, 29]. It remains an interesting question whether some quantum Hall bilayer systems could host this model on the edge through certain modifications such as edge reconstructions [30–32]. In addition, (3.9) realizes the model proposed in Ref. [8] for topological superconducting edge states which exhibit non-Abelian Fibonacci anyonic properties. The model of (2.8) could be viewed as a generalization of their case.

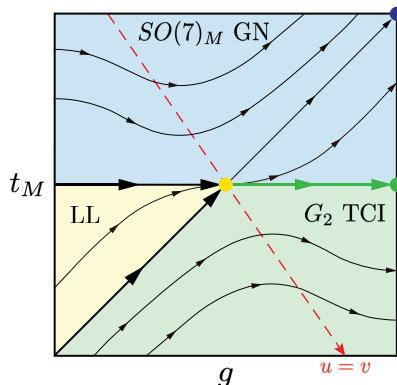


Figure 2. The RG flows and phase diagram on the G_2 critical fixed planes spanned by the G_2 TCI fixed flow and the $SO(7)_M$ critical GN fixed flow. The horizontal and vertical axes are labeled by g and t_M , respectively. The $SO(7)_M$, G_2 TCI, and free Majorana fixed points are denoted by the indigo, green, and yellow dots, respectively. Phase structures in other G_2 critical fixed planes are similar. The embedding of the $u = v$ line in the lattice model is colored in red.

The G_2 TCI fixed flow is special. We can pick up any one GN-type fixed flow together with the G_2 TCI one to form a fixed plane. Consider the interaction Hamiltonian density on such a plane. It can be rearranged as

$$\mathcal{H}_{\text{critical}}^{G_2} = \tilde{g} \sum_{a \neq b} G_{ab}^R G_{ab}^L + \tilde{n} \sum_{a \neq b} \tilde{N}_{ab}^R \tilde{N}_{ab}^L, \quad (3.10)$$

where \tilde{N}_{ab} are the generators of the emergent symmetry on the GN fixed flow. For example, for the $SO(8)_A$ GN fixed flow, $\{\tilde{N}_{ab}^R\} = \{M_{ab}^R, -V_c^R\}$ and $\{\tilde{N}_{ab}^L\} = \{M_{ab}^L, V_c^L\}$ are generators of the $SO(8)_A$ symmetry. Since the emergent symmetry is enlarged including the G_2 as a subgroup, the closure of Lie algebra ensures the RG flow to remain in-plane. The corresponding fixed points (flows) and phases are the GN fixed flow controlling the gapped or critical phase with emergent symmetry, the G_2 TCI fixed flow controlling the G_2 TCI phase, and the free Majorana fixed point controlling the Luttinger liquid phase. As an example, we choose the GN fixed flow as the $SO(7)_M$ critical one. Correspondingly the

fixed plane has $t_A = t_B = 0$, on which the RG equations are reduced to

$$\frac{dg}{dl} = 16g^2 + t_M^2, \quad \frac{dt_M}{dl} = 16gt_M + 2t_M^2. \quad (3.11)$$

It indeed possesses the $SO(7)_M$ critical fixed flow of $t_A = t_B = 0$ and $t_M = 2g \rightarrow +\infty$, or, equivalently, $t = \frac{1}{3}y = -\frac{1}{\sqrt{6}}w = \frac{1}{2}g \rightarrow +\infty$. Along the $SO(7)_M$ critical flow, the interaction Hamiltonian density is reduced to

$$\begin{aligned} \mathcal{H}_{\text{GN}}^{SO(7)_M} &= g \sum_{a \neq b} G_{ab}^R G_{ab}^L + \frac{g}{2} \sum_a T_a^R T_a^L + \frac{3g}{2} \sum_a V_a^R V_a^L - \frac{\sqrt{3}g}{2} \sum_a (T_a^R V_a^L + V_a^R T_a^L) \\ &= g \sum_{a \neq b} M_{ab}^{\prime R} M_{ab}^{\prime L}. \end{aligned} \quad (3.12)$$

The schematic RG flows and the phase diagram on this G_2 critical fixed planes are shown in figure 2. A complete list of fixed flows is given in table 1.

t_A/g	t_B/g	t_M/g	Symmetry	Fixed plane
4/3	4/3	4/3	$SO(8)$	P_A, P_B, P_M
8/3	-4/3	-4/3	$SO(8)_A$	P_A
2	0	0	$SO(7)_A$	P_A
-4/3	8/3	-4/3	$SO(8)_B$	P_B
0	2	0	$SO(7)_B$	P_B
-4/3	-4/3	8/3	$SO(8)_M$	P_M
0	0	2	$SO(7)_M$	P_M
0	0	0	G_2 SUSY	Any

Table 1. Fixed flows ($g \neq 0$), the associated symmetries, and the corresponding fixed planes. P_i ($i = A, B, M$) represents the $SO(7)_i$ symmetric fixed plane. The G_2 TCI fixed flow has emergent supersymmetry endowed by the TCI CFT. In the last row, ‘‘Any’’ means a plane spanned by the G_2 TCI fixed flow and anyone of the GN fixed flows is a fixed plane.

3.3 Phase diagrams in fixed bodies

The transitions between the $SO(8)$ GN phase and each of the $SO(8)_i$ GN phase is revealed by the Ising duality in the corresponding $SO(7)$ fixed plane. Nevertheless, phase transitions between any two of these three $SO(8)_i$ GN phases are more involved, since different stable GN fixed flows are not in the same fixed plane. To investigate this problem, we find the following relation based on the RG equations (3.2),

$$\frac{d\tilde{t}}{dl} = 16g\tilde{t}, \quad (3.13)$$

with $\tilde{t} = t_A + t_B + t_M$. Hence, during the evolution $\tilde{t} = 0$ is maintained. The fixed body spanned by g and $\tilde{t} = 0$ includes all the three $SO(8)_i$ GN fixed flows exhibiting the triality.

The phase diagram in fixed body $\tilde{t} = 0$ is shown in figure 3 (a), which exhibits the D_3 symmetry as a consequence of the triality among the three $SO(8)_i$ phases. The G_2

TCI fixed flow and the free Majorana fixed point also lie in this fixed body, as indicated in table 1. The phase diagram shows that the transition between any two of the three $SO(8)_i$ GN phases is described by either the Luttinger liquid phase with central charge $c = 4$, or, the G_2 TCI phase with central charge $c = \frac{6}{5}$, both of which are actually multi-critical. This coincides with the phenomenon of multiversality that the phase transitions between two phases can have more than one universality classes [16, 17].

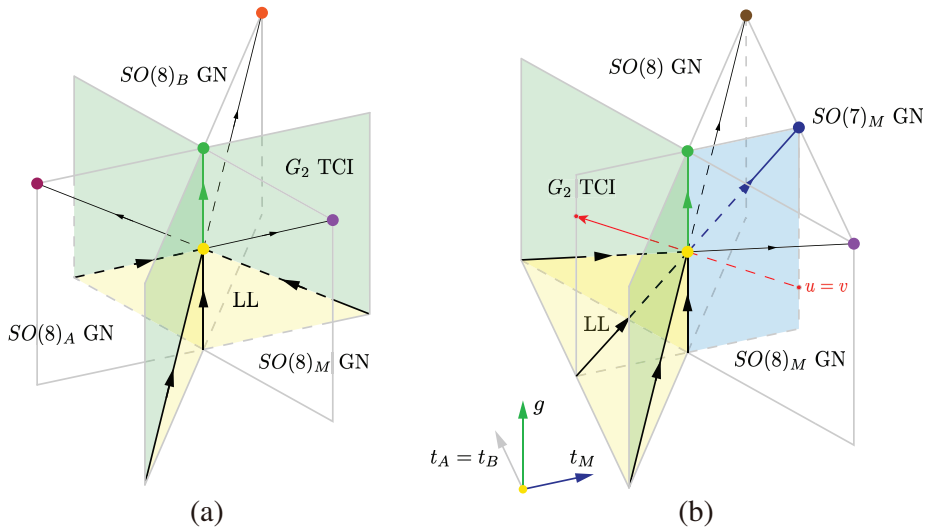


Figure 3. The phase diagrams in the fixed bodies (a) $t = t_A + t_B + t_M = 0$ and (b) $t_A = t_B$. The fixed flows are marked as arrows, and the critical surfaces are colored. In (a), $SO(8)_A$ GN, $SO(8)_B$ GN, $SO(8)_M$ GN, G_2 TCI, and free Majorana fixed points are denoted by crimson, orange, purple, green, and yellow dots, respectively. The transition between each two of the three gapped $SO(8)_i$ GN phases is through either the G_2 TCI phase or the Luttinger liquid (LL) critical phase. The triality relation is manifest in the D_3 symmetry of the phase diagram. In (b), the $SO(8)$ GN, $SO(7)_M$ GN, $SO(8)_M$ GN, G_2 TCI, and free Majorana fixed points are denoted by brown, indigo, purple, green, and yellow dots, respectively. The transition between the $SO(8)$ GN and the $SO(8)_M$ GN phases is through the critical $SO(7)_M$ GN phase in the Ising universality class. The embedding of the $u = v$ axis in the lattice model phase diagram is shown in red, whose positive and negative semi-axes are embedded in the G_2 TCI and the critical $SO(7)_M$ GN phases, respectively.

The RG equations (3.2) also show that if any two of $t_A = t_B = t_M$ are equal, this relation is also maintained during the RG evolution. Hence, there exist another class of three fixed bodies given by $t_A = t_B$, $t_B = t_M$, and $t_M = t_A$, respectively, which are related by triality. As an example, the phase diagram in the fixed body $t_A = t_B$ is shown in figure 3 (b), in which the $SO(7)_M$ fixed plane P_M spanned by three GN fixed flows is embedded.

4 Embedding of the lattice model

Neither triality nor the spacetime supersymmetry survives in the 1D lattice Hubbard-type model of (2.6). It is natural to ask the reason behind such a loss. This is equivalent to investigate the embedding of the lattice model phase diagram into that of the continuum model. The phase diagram of the lattice Hamiltonian (2.6) is spanned by u - and v -axis,

along which the $SO(7)_A$ and $SO(7)_B$ symmetries are restored, respectively. Therefore, the u/v -axis must be a straight line passing the origin point in the $SO(7)_{A/B}$ fixed plane $P_{A/B}$ in the continuum model phase diagram.

A possible embedding of the u -axis is shown in figure 1. According to (3.3), in the parameter space of the continuum model (2.9), the u -axis of the lattice model (2.6) possessing the $SO(7)_A$ symmetry is parameterized as

$$u\text{-axis} : t_A = \left(2 - \frac{k}{2}\right)g, t_B = kg, t_M = kg, \quad (4.1)$$

where k is a constant to be determined. Based on the triality mapping, the v -axis possessing the $SO(7)_B$ symmetry is obtained by switching A and B and fixing M , hence, it is parameterized as

$$v\text{-axis} : t_A = kg, t_B = \left(2 - \frac{k}{2}\right)g, t_M = kg \quad (4.2)$$

Therefore, the phase diagram of the lattice model (2.6) spanned by u -axis and v -axis is given by

$$P_{\text{Lat}} : t_A + t_B = \left(2 + \frac{k}{2}\right)g, t_M = kg. \quad (4.3)$$

To determine the value of k , the $u = v$ axis is checked in the lattice model phase diagram. The lattice Hubbard type interaction (2.6) is invariant under the transformation $\chi_0(i)H_{\text{int}}\chi_0(i) = H_{\text{int}}$ [9]. Hence, χ_0 cannot appear in the local interaction of H_{int} . In other words, χ_0 decouples from other Majorana modes, and hence, the system should be gapless along the entire $u = v$ axis. In P_{Lat} , the $u = v$ axis reads

$$u = v : t_A = t_B = \left(1 + \frac{k}{4}\right)g, t_M = kg, \quad (4.4)$$

which lies in the fixed body $t_A = t_B$. To have both its positive and negative semi-axes embedded in gapless phases, the only choice of k is $k = -4$.

The reasoning why the $SO(7)_M$ is absent in the lattice Hamiltonian (2.6) is presented below. The equation of $SO(7)_M$ fixed plane P_M for the continuum Hamiltonian density is given by $t_A = t_B = 4g - 2t_M$. However, the u - v plane (4.3) of P_{Lat} with $k = -4$ substituted, i.e., $t_A + t_B = 0$ and $t_M = -4g$ is incompatible with the $SO(7)_M$ fixed plane P_M , except the trivial case of $g = t_A = t_B = t_M = 0$, i.e. $u = v = 0$. The triality among three $SO(7)$ symmetries in the continuum model is broken to the duality of $SO(7)_A$ and $SO(7)_B$ on the lattice. This is a reminiscence of triality upon lattice regularization.

We need to figure out how the lattice Hamiltonian (2.6) with $u = v > 0$ and < 0 matches the G_2 critical TCI fixed point and $SO(7)_M$ critical ones, respectively. For the G_2 TCI fixed flow (3.9), the case of $u = v > 0$ of the lattice Hamiltonian should match the case $g > 0$ of the continuum one. Thus the positive semi-axis of $u = v$ should be embedded in the G_2 critical phase, and then naturally the negative semi-axis is embedded in the $SO(7)_M$ critical phase, as shown in figures 2 and 3 (b). Consequently, in the lattice

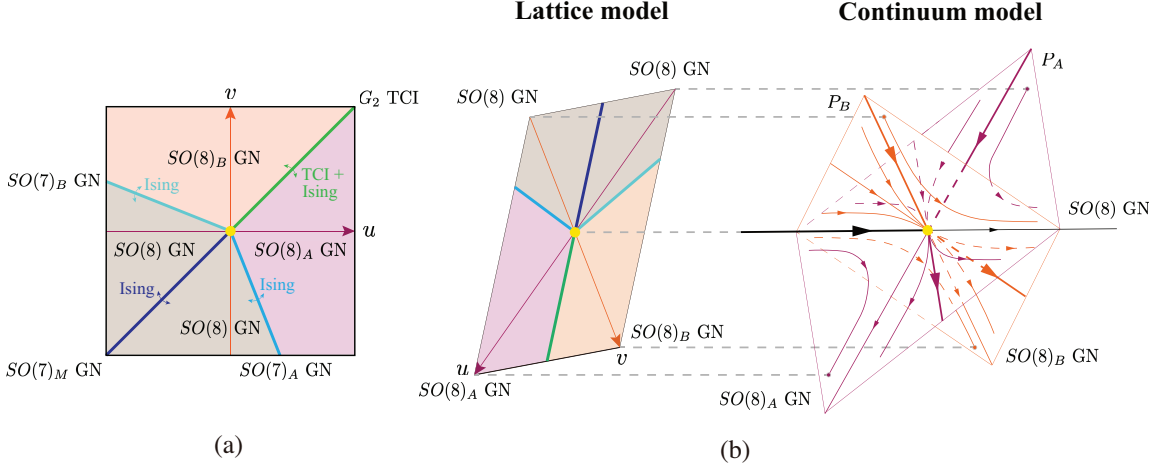


Figure 4. (a) The lattice model phase diagram. There are totally three gapped phases, belonging to $SO(8)_A$ GN, $SO(8)_B$ GN, and $SO(8)$ GN phases in the continuum model. The phase transition between $SO(8)_A$ GN and $SO(8)_B$ GN phases, marked as the green segment, is located at $u = v > 0$, and described by G_2 TCI phase in the continuum model. The phase transition between $SO(8)_A$ ($SO(8)_B$) GN and $SO(8)$ GN phases, represented by the blue (turquoise) segment, is located at $u = -7v$ ($v = -7u$) and belongs to the critical $SO(7)_A$ ($SO(7)_B$) GN phase in the continuum model. Inside the $SO(8)$ GN phase there is a branch cut colored in indigo, on which the system becomes gapless. It is located at $u = v < 0$ and described by the critical $SO(7)_M$ GN phase in the continuum model. (b) Embedding of the lattice model phase diagram into the continuum model phase diagram. RG flows of the continuum model in body $4g - 2t_A - 2t_B + t_M = 0$ (not a fixed body) spanned by $SO(7)_A$ and $SO(7)_B$ symmetric fixed planes (P_A and P_B) are shown in the right. On each $SO(7)$ symmetric fixed plane the RG flows are the same as figure 2 (a) ensured by the triality. The phase boundaries are marked as thick segments. P_A and P_B , as well as RG flows on them, are colored in crimson and orange, respectively. The lattice model phase diagram is shown in the left part. The u/v -axis is embedded in $P_{A/B}$ as a straight line.

model interaction with $u = v > 0$ flows to the G_2 critical TCI fixed point, and that of $u = v < 0$ flows to the $SO(7)_M$ critical fixed point.

The phase diagram of the lattice model Hamiltonian (2.6) is shown in figure 4 (a), supplemented by a numerical integration of the RG equations on the embedded lattice model phase diagram $P_{\text{Lat}} : t_A + t_B = 0, t_M = -4g$ (see appendix D for details). The Ising transition line between $SO(8)_A$ ($SO(8)_B$) GN phase and $SO(8)$ GN phase is located at $u = -7v$ ($v = -7u$), which perfectly agrees with the mean-field analysis of the lattice model [9]. The embedding of the lattice phase diagram is shown in figure 4 (b). The u -axis possesses the $SO(7)_A$ symmetry. Compared to the phase diagram of the continuum model shown in figure 1, the sign of g in the continuum Hamiltonian density follows that of u , while that of y is opposite to u . Hence, the positive u -axis is embedded in the $SO(8)_A$ GN phase, and its negative axis is embedded in the $SO(8)$ GN phase. By the triality mapping, the positive v -axis is embedded in the $SO(8)_B$ GN phase, and the negative v -axis is also in the $SO(8)$ GN phase.

For the $u = v$ axis, its negative semi-axis ($u = v < 0$) embedded in the critical $SO(7)_M$

GN phase is a branch cut lying inside the gapped $SO(8)$ GN phase. Its gaplessness is due to the decoupled free Majorana χ_0 , which is consistent with the analysis of the $u = v$ axis in the lattice model [9]. This criticality sandwiched in the same phase is an example of the unnecessary criticality [16, 17]. On the other hand, the positive $u = v$ semi-axis, embedded in the G_2 critical phase, describes the transition between $SO(8)_A$ GN and $SO(8)_B$ GN phases in the lattice model. Such a transition on lattice inherits the universality class and the central charge $c = \frac{7}{10} + \frac{1}{2}$ of the G_2 TCI phase in the continuum.

The spacetime supersymmetry in the G_2 TCI phase also has a reminiscence on the lattice. For a CFT with $\mathcal{N} = 1$ spacetime supersymmetry, the primary fields come in pairs. Within each pair the two primary fields have scaling dimension differed by $\frac{1}{2}$, and hence can be viewed as the supersymmetry partner of each other. For example, for the TCI CFT described by (3.9), the stress-energy tensor for right-mover $T_B^R \sim C_{abcd}\chi_{a+1}^R\chi_{b+1}^R\chi_{c+1}^R\chi_{d+1}^R$ with scaling dimension 2 has a supersymmetry partner $T_F^R \sim C_{abc}\chi_{a+1}^R\chi_{b+1}^R\chi_{c+1}^R$ with scaling dimension $\frac{3}{2}$ [13] (this operator is also called ϵ'' in CFT literature). Typically, a lattice model with low energy effective theory governed by a supersymmetric CFT exhibits quantum mechanical supersymmetry [33, 34]. Similar to the supersymmetric CFT, in a lattice model with $\mathcal{N} = 1$ quantum mechanical supersymmetry, the eigenstates of the Hamiltonian H_{SUSY} also come in pairs, within which the two states have different fermion parity and related to each other by a supercharge operator Q satisfying $H_{\text{SUSY}} = Q^2$. This phenomenon particularly resembles the G_2 invariant lattice model (2.6) when $u = v$, which exhibits the degeneracy between bosonic and fermionic states on each site [9]. The “supercharge operator” switching bosonic and fermionic states on site i is just the Majorana operator $\chi_0(i)$. However, this is not an authentic supersymmetry since $H_{\text{int}}^{G_2} \neq (\sum_i \chi_0(i))^2$, and hence does not satisfy the definition of the quantum mechanical supersymmetry. Nevertheless, this degeneracy between on-site bosonic and fermionic states can still be viewed as the lattice reminiscence of the spacetime supersymmetry in the continuum model.

5 Conclusions

In summary, we investigate the low energy effective theory of the minimal G_2 symmetric lattice model [9] in (1+1)D by an one-loop RG method. The $SO(8)$ triality, which is absent in the lattice model due to the on-site Hubbard-type interactions, emerges naturally in the low energy effective theory as a triality mapping among three different $SO(7)$ symmetries, and consequently three gapped phases as well as three Ising critical phases. The phase transitions between phases related by the triality relation are unified by either a Luttinger liquid phase, or a G_2 symmetric multi-critical phase. This G_2 multi-critical phase is described by a direct product of Ising and TCI CFTs with central charge $c = \frac{1}{2} + \frac{7}{10} = \frac{6}{5}$, and possesses emergent spacetime supersymmetry carried by the TCI CFT. When the continuum model is regularized on a lattice, the triality among three $SO(7)$ symmetries is broken to the duality of two $SO(7)$ symmetries [9], eliminating the third one. The spacetime supersymmetry is also degraded to a degeneracy pattern between the on-site bosonic and fermionic states, instead of an authentic quantum mechanical supersymmetry. How-

ever, these reminiscences in ultraviolet still imply clues of exotic structures in infrared, as explored in the current work.

Acknowledgments

ZQG acknowledges D.-H. Lee, H. Yang, Y.-Q. Wang, Z. Han, and J.-C. Feng for helpful discussions. CW is supported by the National Natural Science Foundation of China under the Grant No. 12234016 and No. 12174317. This work has been supported by the New Cornerstone Science Foundation.

References

- [1] A.B. Zamolodchikov, *Integrals of motion and s-matrix of the (scaled) $t = tc$ ising model with magnetic field*, *International Journal of Modern Physics A* **04** (1989) 4235.
- [2] R. Coldea, D. Tennant, E. Wheeler, E. Wawrzynska, D. Prabhakaran, M. Telling et al., *Quantum criticality in an ising chain: Experimental evidence for emergent $e8$ symmetry*, *Science* **327** (2010) 177.
- [3] B.A. Bernevig, J. Hu, N. Toumbas and S.-C. Zhang, *Eight-dimensional quantum hall effect and “octonions”*, *Phys. Rev. Lett.* **91** (2003) 236803.
- [4] P.L.S. Lopes, V.L. Quito, B. Han and J.C.Y. Teo, *Non-abelian twist to integer quantum hall states*, *Phys. Rev. B* **100** (2019) 085116.
- [5] A. Kitaev, *Anyons in an exactly solved model and beyond*, *Annals of Physics* **321** (2006) 2.
- [6] I. Agricola, *Old and new on the exceptional group G_2* , *Notices Amer. Math. Soc.* **55** (2008) 922.
- [7] J.C. Baez, *The octonions*, *Bull. Am. Math. Soc* **39** (2002) 145.
- [8] Y. Hu and C.L. Kane, *Fibonacci topological superconductor*, *Phys. Rev. Lett.* **120** (2018) 066801.
- [9] Z.-Q. Gao and C. Wu, *Exceptional symmetry of g_2 in spin- $\frac{3}{2}$ fermion systems*, *ArXiv e-prints* (2020) [[2010.14126](#)].
- [10] Y.-M. Zhan, Y.-G. Chen, B. Chen, Z. Wang, Y. Yu and X. Luo, *Universal topological quantum computation with strongly correlated majorana edge modes*, *New Journal of Physics* **24** (2022) 043009.
- [11] C. Li, V.L. Quito, D. Schuricht and P.L.S. Lopes, *G_2 integrable point characterization via isotropic spin-3 chains*, *Phys. Rev. B* **108** (2023) 165123.
- [12] A. Rahmani, X. Zhu, M. Franz and I. Affleck, *Emergent supersymmetry from strongly interacting majorana zero modes*, *Phys. Rev. Lett.* **115** (2015) 166401.
- [13] S.L. Shatashvili and C. Vafa, *Superstrings and manifolds of exceptional holonomy*, *Selecta Mathematica* **1** (1995) 347.
- [14] D. Friedan, Z. Qiu and S. Shenker, *Superconformal invariance in two dimensions and the tricritical ising model*, *Physics Letters B* **151** (1985) 37.
- [15] Z. Qiu, *Supersymmetry, two-dimensional critical phenomena and the tricritical ising model*, *Nuclear Physics B* **270** (1986) 205.

- [16] Z. Bi and T. Senthil, *Adventure in topological phase transitions in 3 + 1-d: Non-abelian deconfined quantum criticalities and a possible duality*, *Phys. Rev. X* **9** (2019) 021034.
- [17] A. Prakash, M. Fava and S.A. Parameswaran, *Multiversality and unnecessary criticality in one dimension*, *Phys. Rev. Lett.* **130** (2023) 256401.
- [18] C. Wu, J.P. Hu and S.C. Zhang, *Exact $so(5)$ symmetry in the spin-3/2 fermionic system*, *Phys. Rev. Lett.* **91** (2003) 186402.
- [19] C. Wu, *Hidden symmetry and quantum phases in spin-3/2 cold atomic systems*, *Modern Physics Letters B* **20** (2006) 1707.
- [20] M. Günaydin and S.V. Ketov, *Seven-sphere and the exceptional $n = 7$ and $n = 8$ superconformal algebras*, *Nuclear Physics B* **467** (1996) 215.
- [21] R. Shankar, *Solvable models with self-triality in statistical mechanics and field theory*, *Physical Review Letters* **46** (1981) 379.
- [22] H.-H. Lin, L. Balents and M.P.A. Fisher, *Exact $so(8)$ symmetry in the weakly-interacting two-leg ladder*, *Physical Review B* **58** (1998) 1794.
- [23] L. Fidkowski and A. Kitaev, *Effects of interactions on the topological classification of free fermion systems*, *Physical Review B* **81** (2010) .
- [24] D.J. Gross and A. Neveu, *Dynamical symmetry breaking in asymptotically free field theories*, *Physical Review D* **10** (1974) 3235.
- [25] C. Wu, *Competing orders in one dimensional spin 3/2 fermionic systems*, *Phys. Rev. Lett.* **95** (2005) 266404.
- [26] E. Fradkin, *Field Theories of Condensed Matter Physics*, Cambridge University Press, 2 ed. (2013).
- [27] M. Ninomiya and K. Yamagishi, *Nonlocal $su(3)$ current algebra*, *Physics Letters B* **183** (1987) 323.
- [28] E. Ardonne and K. Schoutens, *Wavefunctions for topological quantum registers*, *Annals of Physics* **322** (2007) 201.
- [29] E. Grosfeld and K. Schoutens, *Non-abelian anyons: When ising meets fibonacci*, *Physical Review Letters* **103** (2009) .
- [30] S.M. Girvin, *Particle-hole symmetry in the anomalous quantum hall effect*, *Physical Review B* **29** (1984) 6012.
- [31] A.H. MacDonald, *Edge states in the fractional-quantum-hall-effect regime*, *Physical Review Letters* **64** (1990) 220.
- [32] C.L. Kane, M.P.A. Fisher and J. Polchinski, *Randomness at the edge: Theory of quantum hall transport at filling $\nu=2/3$* , *Physical Review Letters* **72** (1994) 4129.
- [33] P. Fendley, K. Schoutens and J. de Boer, *Lattice models with $\mathcal{N} = 2$ supersymmetry*, *Phys. Rev. Lett.* **90** (2003) 120402.
- [34] C. Li, E. Lantagne-Hurtubise and M. Franz, *Supersymmetry in an interacting majorana model on the kagome lattice*, *Phys. Rev. B* **100** (2019) 195146.

A Fermion bilinears and majorana operators in the lattice model

Define four by four gamma matrices as

$$\Gamma^1 = \begin{pmatrix} 0 & -iI \\ iI & 0 \end{pmatrix}, \quad \Gamma^{2,3,4} = \begin{pmatrix} \vec{\sigma} & 0 \\ 0 & -\vec{\sigma} \end{pmatrix}, \quad \Gamma^5 = \begin{pmatrix} 0 & I \\ I & 0 \end{pmatrix}, \quad (\text{A.1})$$

where I and $\vec{\sigma}$ are two by two identity and Pauli matrices. These five gamma matrices form an $Sp(4)$ vector. The generators of $Sp(4)$ are defined as $\Gamma^{ab} = -\frac{i}{2}[\Gamma^a, \Gamma^b]$, and the charge conjugation operator is defined as $R = \Gamma^1\Gamma^3$. Therefore, the fermion bilinears on each site i , $N_{ab}(i)$ with $0 \leq a, b \leq 7$, spanning an $SO(8)$ algebra reads

$$N_{ab}(i) = -\frac{1}{2}\psi^\dagger(i)\Gamma^{ab}\psi(i), \quad 1 \leq a, b \leq 5, \quad (\text{A.2})$$

$$N_{a7}(i) = \frac{1}{2}\psi^\dagger(i)\Gamma^a\psi(i), \quad 1 \leq a \leq 5, \quad (\text{A.3})$$

$$N_{06}(i) = \frac{1}{2}\psi^\dagger(i)\psi(i) - 1, \quad (\text{A.4})$$

$$N_{0a}(i) + iN_{a6}(i) = -\frac{i}{2}\text{sgn}(i)\psi^\dagger(i)\Gamma^a R\psi^\dagger(i), \quad 1 \leq a \leq 5, \quad (\text{A.5})$$

$$N_{07}(i) - iN_{67}(i) = \frac{1}{2}\text{sgn}(i)\psi^\dagger(i)R\psi^\dagger(i), \quad (\text{A.6})$$

where $\text{sgn}(i) = \pm 1$ is staggered on two sublattices of the bipartite lattice. The Majorana operators, transformed under the vector representation of $SO(8)$, are defined as

$$\begin{aligned} \chi_1(i) &= e^{-i\text{sgn}(i)\pi/4}\psi_{\frac{1}{2}}(i) + e^{i\text{sgn}(i)\pi/4}\psi_{\frac{1}{2}}^\dagger(i), \\ \chi_2(i) &= -e^{i\text{sgn}(i)\pi/4}\psi_{\frac{1}{2}}(i) - e^{-i\text{sgn}(i)\pi/4}\psi_{\frac{1}{2}}^\dagger(i), \\ \chi_3(i) &= e^{-i\text{sgn}(i)\pi/4}\psi_{-\frac{1}{2}}(i) + e^{i\text{sgn}(i)\pi/4}\psi_{-\frac{1}{2}}^\dagger(i), \\ \chi_4(i) &= -e^{i\text{sgn}(i)\pi/4}\psi_{\frac{3}{2}}(i) - e^{-i\text{sgn}(i)\pi/4}\psi_{\frac{3}{2}}^\dagger(i), \\ \chi_5(i) &= e^{i\text{sgn}(i)\pi/4}\psi_{-\frac{1}{2}}(i) + e^{-i\text{sgn}(i)\pi/4}\psi_{-\frac{1}{2}}^\dagger(i), \\ \chi_6(i) &= e^{-i\text{sgn}(i)\pi/4}\psi_{-\frac{3}{2}}(i) + e^{i\text{sgn}(i)\pi/4}\psi_{-\frac{3}{2}}^\dagger(i), \\ \chi_7(i) &= e^{i\text{sgn}(i)\pi/4}\psi_{-\frac{3}{2}}(i) + e^{-i\text{sgn}(i)\pi/4}\psi_{-\frac{3}{2}}^\dagger(i), \\ \chi_0(i) &= e^{-i\text{sgn}(i)\pi/4}\psi_{\frac{3}{2}}(i) + e^{i\text{sgn}(i)\pi/4}\psi_{\frac{3}{2}}^\dagger(i), \end{aligned} \quad (\text{A.7})$$

where $\chi_1(i) \sim \chi_7(i)$ form a G_2 vector while $\chi_0(i)$ is a G_2 singlet. In fact, $\chi_1(i) \sim \chi_7(i)$ also form a vector of $SO(7)_M$ spanned by $i\chi_m(i)\chi_n(i)$ with $1 \leq m, n \leq 7$, which is absent in the lattice model. The G_2 weights of these Majorana fermions are given in table 2. As a comparison, the weight of bosonic and fermionic states are also listed.

Weight μ	Bosonic vector	Fermionic vector	Majorana vector
$(\frac{\sqrt{3}}{2}, \frac{1}{2})$	$\psi_{\frac{1}{2}}^\dagger \psi_{-\frac{3}{2}}^\dagger 0\rangle$	$\psi_{\frac{3}{2}}^\dagger \psi_{\frac{1}{2}}^\dagger \psi_{-\frac{3}{2}}^\dagger 0\rangle$	$\frac{1}{2}(\chi_1 + i\chi_2)$
$(0, 1)$	$\psi_{\frac{3}{2}}^\dagger \psi_{\frac{1}{2}}^\dagger \psi_{-\frac{1}{2}}^\dagger \psi_{-\frac{3}{2}}^\dagger 0\rangle$	$\psi_{\frac{1}{2}}^\dagger \psi_{-\frac{1}{2}}^\dagger \psi_{-\frac{3}{2}}^\dagger 0\rangle$	$\frac{1}{2}(\chi_6 - i\chi_7)$
$(-\frac{\sqrt{3}}{2}, \frac{1}{2})$	$\psi_{-\frac{1}{2}}^\dagger \psi_{-\frac{3}{2}}^\dagger 0\rangle$	$\psi_{\frac{3}{2}}^\dagger \psi_{-\frac{1}{2}}^\dagger \psi_{-\frac{3}{2}}^\dagger 0\rangle$	$\frac{1}{2}(\chi_3 - i\chi_5)$
$(-\frac{\sqrt{3}}{2}, -\frac{1}{2})$	$\psi_{\frac{3}{2}}^\dagger \psi_{-\frac{1}{2}}^\dagger 0\rangle$	$\psi_{-\frac{1}{2}}^\dagger 0\rangle$	$\frac{1}{2}(\chi_1 - i\chi_2)$
$(0, -1)$	$ 0\rangle$	$\psi_{\frac{3}{2}}^\dagger 0\rangle$	$\frac{1}{2}(\chi_6 + i\chi_7)$
$(\frac{\sqrt{3}}{2}, -\frac{1}{2})$	$\psi_{\frac{3}{2}}^\dagger \psi_{\frac{1}{2}}^\dagger 0\rangle$	$\psi_{\frac{1}{2}}^\dagger 0\rangle$	$\frac{1}{2}(\chi_3 + i\chi_5)$
$(0, 0)$	$\frac{1}{\sqrt{2}}(\psi_{\frac{3}{2}}^\dagger \psi_{-\frac{3}{2}}^\dagger + \psi_{\frac{1}{2}}^\dagger \psi_{-\frac{1}{2}}^\dagger) 0\rangle$	$\frac{1}{\sqrt{2}}(\psi_{-\frac{3}{2}}^\dagger \pm i\psi_{\frac{3}{2}}^\dagger \psi_{\frac{1}{2}}^\dagger \psi_{-\frac{1}{2}}^\dagger) 0\rangle$	χ_4
Weight μ	Bosonic singlet	Fermionic singlet	Majorana singlet
$(0, 0)$	$\frac{1}{\sqrt{2}}(\psi_{\frac{3}{2}}^\dagger \psi_{-\frac{3}{2}}^\dagger - \psi_{\frac{1}{2}}^\dagger \psi_{-\frac{1}{2}}^\dagger) 0\rangle$	$\frac{1}{\sqrt{2}}(\psi_{-\frac{3}{2}}^\dagger \mp i\psi_{\frac{3}{2}}^\dagger \psi_{\frac{1}{2}}^\dagger \psi_{-\frac{1}{2}}^\dagger) 0\rangle$	χ_0

Table 2. Bosonic states, fermionic states, and Majorana operators classified by G_2 weight. The \pm signs in the $(0, 0)$ weight states are staggered on sublattices. The site label is omitted for clarity.

In this Majorana basis, the lattice Hamiltonian reads (constant term neglected)

$$\begin{aligned}
H_0 &= \frac{it_{\text{hop}}}{2} \left(\sum_i \chi_0(i)\chi_0(i+1) + \chi_1(i)\chi_1(i+1) + \chi_3(i)\chi_3(i+1) + \chi_6(i)\chi_6(i+1) \right) \\
&\quad - \frac{it_{\text{hop}}}{2} \left(\sum_i \chi_2(i)\chi_2(i+1) + \chi_4(i)\chi_4(i+1) + \chi_5(i)\chi_5(i+1) + \chi_7(i)\chi_7(i+1) \right), \\
H_{\text{int}}^{G_2} &= \frac{u-v}{8} \sum_i \chi_0(i) C_{abc} \chi_{a+1}(i) \chi_{b+1}(i) \chi_{c+1}(i) \\
&\quad - \frac{u+v}{32} \sum_i C_{abcd} \chi_{a+1}(i) \chi_{b+1}(i) \chi_{c+1}(i) \chi_{d+1}(i), \tag{A.8}
\end{aligned}$$

where the structure constant of octonions C_{abc} is chosen as $C_{031} = C_{052} = C_{064} = C_{126} = C_{154} = C_{243} = C_{365} = 1$ with dual tensor $C_{ijkl} = \frac{1}{6} \epsilon_{ijkl} C_{abc}$. When $u = v$, the interaction Hamiltonian reads

$$H_{\text{int}}^{G_2} = \frac{3}{2} u \sum_i G_{ab}(i)^2 = -\frac{u}{16} \sum_i C_{abcd} \chi_{a+1}(i) \chi_{b+1}(i) \chi_{c+1}(i) \chi_{d+1}(i), \tag{A.9}$$

from which it can be seen that only 7 out of 8 Majoranas, except for $\chi_0(i)$, appear in this Hamiltonian.

B RG equations

The current algebras read (constant terms neglected since they do not contribute to the RG equations)

$$G_{ab}^R(z)G_{cd}^R(w) \sim \frac{1}{z-w} \left(\frac{2}{3}\delta_{ac}G_{bd}^R(w) + \frac{2}{3}\delta_{bd}G_{ac}^R(w) - \frac{2}{3}\delta_{ad}G_{bc}^R(w) - \frac{2}{3}\delta_{ac}G_{bd}^R(w) \right. \\ \left. + \frac{1}{6}C_{bcam}G_{md}^R(w) + \frac{1}{6}C_{dabm}G_{mc}^R(w) - \frac{1}{6}C_{bcdm}G_{ma}^R(w) - \frac{1}{6}C_{dacm}G_{mb}^R(w) \right) \quad (\text{B.1})$$

$$G_{ab}^R(z)T_c^R(w) \sim \frac{1}{z-w} \left(\frac{2}{3}\delta_{bc}T_a^R(w) - \frac{2}{3}\delta_{ac}T_b^R(w) + \frac{1}{3}C_{abcd}T_d^R(w) \right), \quad (\text{B.2})$$

$$G_{ab}^R(z)V_c^R(w) \sim \frac{1}{z-w} \left(\frac{2}{3}\delta_{bc}V_a^R(w) - \frac{2}{3}\delta_{ac}V_b^R(w) + \frac{1}{3}C_{abcd}V_d^R(w) \right), \quad (\text{B.3})$$

$$T_a^R(z)T_b^R(w) \sim \frac{1}{z-w} \left(-G_{ab}^R(w) + \frac{1}{\sqrt{3}}C_{abc}T_c^R(w) \right), \quad (\text{B.4})$$

$$T_a^R(z)V_b^R(w) \sim \frac{1}{z-w} \left(-\frac{1}{\sqrt{3}}C_{abc}V_c^R(w) \right), \quad (\text{B.5})$$

$$V_a^R(z)V_b^R(w) \sim \frac{1}{z-w} \left(-G_{ab}^R(w) - \frac{1}{\sqrt{3}}C_{abc}T_c^R(w) \right), \quad (\text{B.6})$$

and for left-handed currents the current algebra is the same, except for z substituted by \bar{z} . The WZW level is irrelevant to the one-loop RG of interaction Hamiltonian density, so it is simply dropped. Consider operator product expansions (OPE) showing up in the calculation of one-loop RG as follows.

1.

$$G_{ab}^R(z)G_{ab}^L(\bar{z})G_{cd}^R(w)G_{cd}^L(\bar{w}) \sim \frac{1}{|z-w|^2} \frac{4}{9} \left(\delta \cdot G^R + \frac{1}{4}C \cdot G^R \right) \left(\delta \cdot G^L + \frac{1}{4}C \cdot G^L \right) \quad (\text{B.7})$$

where shorthands $\delta \cdot G$ and $C \cdot G$ are used to represent four δ -terms and four C -terms in (B.1) for simplicity. Consider $(\delta \cdot G^R)(\delta \cdot G^L)$ first.

$$\begin{aligned} (\delta \cdot G^R)(\delta \cdot G^L) &= (\delta_{ac}G_{bd}^R + \delta_{bd}G_{ac}^R - \delta_{ad}G_{bc}^R - \delta_{ac}G_{bd}^R)(\delta_{ac}G_{bd}^L + \delta_{bd}G_{ac}^L - \delta_{ad}G_{bc}^L - \delta_{ac}G_{bd}^L) \\ &= -2\delta_{ad}\delta_{ac}G_{bc}^R G_{bd}^L - 2\delta_{ad}\delta_{bd}G_{bc}^R G_{ac}^L - 2\delta_{bc}\delta_{ac}G_{ad}^R G_{bd}^L - 2\delta_{bc}\delta_{bd}G_{ad}^R G_{ac}^L \\ &\quad - 2\delta_{bc}\delta_{ac}G_{ad}^R G_{bd}^L + 2\delta_{ad}\delta_{bc}G_{bc}^R G_{ad}^L + 2\delta_{ac}\delta_{bd}G_{ac}^R G_{bd}^L + 4\delta_{cd}\delta_{cd}G_{ab}^R G_{ab}^L \\ &= -2 \times 4G_{ab}^R G_{ab}^L + 0 + 4 \times 7G_{ab}^R G_{ab}^L \\ &= 20G_{ab}^R G_{ab}^L, \end{aligned} \quad (\text{B.8})$$

where identities $G_{ab} = -G_{ba}$, $\delta_{ab}G_{ab} = 0$ and $\delta_{ab}\delta_{ab} = 7$ are employed in passing to the third equality. Then consider $(C \cdot G^R)(C \cdot G^L)$.

$$\begin{aligned} (C \cdot G^R)(C \cdot G^L) &= 4C_{dacm}G_{mb}^R C_{dacn}G_{nb}^L + 4C_{dacm}G_{mb}^R C_{dabn}G_{nc}^L \\ &= 4 \times 24\delta_{mn}G_{mb}^R G_{nb}^L + 4 \times (-2C_{cmbn} + 4(\delta_{cb}\delta_{mn} - \delta_{cn}\delta_{bm}))G_{mb}^R G_{nc}^L \\ &= 96G_{ab}^R G_{ab}^L + 8C_{abcd}G_{ab}^R G_{cd}^L + 4G_{ab}^R G_{ab}^L - 4 \times 0 \\ &= 96G_{ab}^R G_{ab}^L + 16G_{ab}^R G_{ab}^L + 16G_{ab}^R G_{ab}^L \\ &= 128G_{ab}^R G_{ab}^L, \end{aligned} \quad (\text{B.9})$$

where identities $C_{mnab}C_{mncd} = -2C_{abcd} + 4(\delta_{ac}\delta_{bd} - \delta_{ad}\delta_{bc})$ and $C_{abcm}C_{abcn} = 24\delta_{mn}$ are employed in the second equality, and identities $C_{abcd}G_{cd} = 2G_{ab}$ and $G_{ab} = -G_{ba}$ are employed in the fourth equality. Then consider $(\delta \cdot G^R)(C \cdot G^L) + (C \cdot G^R)(\delta \cdot G^L)$.

$$\begin{aligned}
(\delta \cdot G^R)(C \cdot G^L) + (C \cdot G^R)(\delta \cdot G^L) &= 4C_{dacm}G_{mc}^R G_{ad}^L + 4C_{bcam}G_{mb}^R G_{ac}^L \\
&\quad - 4C_{dacm}G_{ma}^R G_{cd}^L - 4C_{bcam}G_{bc}^R G_{ma}^L \\
&= 4 \times 4C_{abcd}G_{ab}^R G_{cd}^L \\
&= 32G_{ab}^R G_{ab}^L,
\end{aligned} \tag{B.10}$$

where identities $\delta_{ab}C_{abcd} = 0$ and $C_{abcd}G_{cd} = 2G_{ab}$ are employed. In summary, the OPE of $G_{ab}^R(z)G_{ab}^L(\bar{z})G_{cd}^R(w)G_{cd}^L(\bar{w})$ gives rise to

$$\begin{aligned}
G_{ab}^R(z)G_{ab}^L(\bar{z})G_{cd}^R(w)G_{cd}^L(\bar{w}) &\sim \frac{1}{|z-w|^2} \frac{4}{9} \left(20 + \frac{1}{16} \times 128 + \frac{1}{4} \times 32 \right) G_{ab}^R G_{ab}^L \\
&= \frac{1}{|z-w|^2} 16G_{ab}^R G_{ab}^L.
\end{aligned} \tag{B.11}$$

2.

$$\begin{aligned}
T_a^R(z)T_a^L(\bar{z})T_b^R(w)T_b^L(\bar{w}) &\sim \frac{1}{|z-w|^2} \left(-G_{ab}^R + \frac{1}{\sqrt{3}}C_{abc}T_c^R \right) \left(-G_{ab}^L + \frac{1}{\sqrt{3}}C_{abd}T_d^L \right) \\
&= \frac{1}{|z-w|^2} (G_{ab}^R G_{ab}^L + 2T_a^R T_a^L),
\end{aligned} \tag{B.12}$$

where identities $C_{abc}G_{bc} = 0$ and $C_{abc}C_{abd} = 6\delta_{cd}$ are employed.

3.

$$\begin{aligned}
V_a^R(z)V_a^L(\bar{z})V_b^R(w)V_b^L(\bar{w}) &\sim \frac{1}{|z-w|^2} \left(-G_{ab}^R - \frac{1}{\sqrt{3}}C_{abc}T_c^R \right) \left(-G_{ab}^L - \frac{1}{\sqrt{3}}C_{abd}T_d^L \right) \\
&= \frac{1}{|z-w|^2} (G_{ab}^R G_{ab}^L + 2T_a^R T_a^L),
\end{aligned} \tag{B.13}$$

where identities $C_{abc}G_{bc} = 0$ and $C_{abc}C_{abd} = 6\delta_{cd}$ are employed.

4.

$$\begin{aligned}
G_{ab}^R(z)G_{ab}^L(\bar{z})T_c^R(w)T_c^L(\bar{w}) &\sim \frac{1}{|z-w|^2} \left(\frac{2}{3}\delta_{bc}T_a^R - \frac{2}{3}\delta_{ac}T_b^R + \frac{1}{3}C_{abcd}T_d^R \right) \\
&\quad \times \left(\frac{2}{3}\delta_{bc}T_a^L - \frac{2}{3}\delta_{ac}T_b^L + \frac{1}{3}C_{abce}T_e^L \right) \\
&= \frac{1}{|z-w|^2} \left(\frac{4}{9}(\delta_{bc}T_a^R - \delta_{ac}T_b^R)(\delta_{bc}T_a^L - \delta_{ac}T_b^L) \right. \\
&\quad \left. + \frac{1}{9}C_{abcd}C_{abce}T_d^R T_e^L \right) \\
&= \frac{1}{|z-w|^2} \frac{1}{9} (4 \times 2 \times 7T_a^R T_a^L - 4 \times 2T_a^R T_a^L + 24\delta_{de}T_d^R T_e^L) \\
&= \frac{1}{|z-w|^2} 8T_a^R T_a^L,
\end{aligned} \tag{B.14}$$

where identities $\delta_{ab}\delta_{ab} = 7$, $\delta_{ab}C_{abcd} = 0$ and $C_{abcm}C_{abcn} = 24\delta_{mn}$ are employed. Since both T_a and V_a forms G_2 vector representations, the result above can be directly generalized to the OPE below:

$$G_{ab}^R(z)G_{ab}^L(\bar{z})V_c^R(w)V_c^L(\bar{w}) \sim \frac{1}{|z-w|^2}8V_a^RV_a^L, \quad (\text{B.15})$$

$$G_{ab}^R(z)G_{ab}^L(\bar{z})(V_c^R(w)T_c^L(\bar{w}) + T_c^R(w)V_c^L(\bar{w})) \sim \frac{1}{|z-w|^2}8(V_a^RT_a^L + T_a^RV_a^L). \quad (\text{B.16})$$

5.

$$\begin{aligned} T_a^R(z)T_a^L(\bar{z})V_b^R(w)V_b^L(\bar{w}) &\sim \frac{1}{|z-w|^2}\frac{1}{3}C_{abc}C_{abd}V_c^RV_d^L \\ &= \frac{1}{|z-w|^2}\frac{1}{3} \times 6\delta_{cd}V_c^RV_d^L \\ &= \frac{1}{|z-w|^2}2V_a^RV_a^L. \end{aligned} \quad (\text{B.17})$$

6.

$$\begin{aligned} &(V_a^R(z)T_a^L(\bar{z}) + T_a^R(z)V_a^L(\bar{z}))(V_b^R(w)T_b^L(\bar{w}) + T_b^R(w)V_b^L(\bar{w})) \\ &\sim \frac{1}{|z-w|^2}2\left(\left(-G_{ab}^R + \frac{1}{\sqrt{3}}C_{abc}T_c^R\right)\left(-G_{ab}^L - \frac{1}{\sqrt{3}}C_{abd}T_d^L\right)\right. \\ &+ \left.2\left(-\frac{1}{\sqrt{3}}C_{abc}V_c^R\right)\left(-\frac{1}{\sqrt{3}}C_{abd}V_d^L\right)\right) \\ &= \frac{1}{|z-w|^2}(2G_{ab}^RG_{ab}^L - 4T_a^RT_a^L + 4V_a^RV_a^L), \end{aligned} \quad (\text{B.18})$$

where identities $C_{abc}G_{bc} = 0$ and $C_{abc}C_{abd} = 6\delta_{cd}$ are employed.

7.

$$\begin{aligned} &T_a^R(z)T_a^L(\bar{z})(V_b^R(w)T_b^L(\bar{w}) + T_b^R(w)V_b^L(\bar{w})) \\ &\sim \frac{1}{|z-w|^2}\left(\left(-G_{ab}^R + \frac{1}{\sqrt{3}}C_{abc}T_c^R\right)\left(-\frac{1}{\sqrt{3}}C_{abd}V_d^L\right)\right. \\ &+ \left.\left(-\frac{1}{\sqrt{3}}C_{abc}V_c^R\right)\left(-G_{ab}^L - \frac{1}{\sqrt{3}}C_{abd}T_d^L\right)\right) \\ &= \frac{1}{|z-w|^2}(-2(V_a^RT_a^L + T_a^RV_a^L)), \end{aligned} \quad (\text{B.19})$$

where identities $C_{abc}G_{bc} = 0$ and $C_{abc}C_{abd} = 6\delta_{cd}$ are employed.

8.

$$\begin{aligned} &V_a^R(z)V_a^L(\bar{z})(V_b^R(w)T_b^L(\bar{w}) + T_b^R(w)V_b^L(\bar{w})) \\ &\sim \frac{1}{|z-w|^2}\left(\left(-G_{ab}^R - \frac{1}{\sqrt{3}}C_{abc}T_c^R\right)\left(-\frac{1}{\sqrt{3}}C_{abd}V_d^L\right)\right. \\ &- \left.\left(-\frac{1}{\sqrt{3}}C_{abc}V_c^R\right)\left(-G_{ab}^L - \frac{1}{\sqrt{3}}C_{abd}T_d^L\right)\right) \\ &= \frac{1}{|z-w|^2}2(V_a^RT_a^L + T_a^RV_a^L), \end{aligned} \quad (\text{B.20})$$

where identities $C_{abc}G_{bc} = 0$ and $C_{abc}C_{abd} = 6\delta_{cd}$ are employed.

Combine the results of OPE 1 \sim 8. The OPE of interaction Hamiltonian density reads

$$\begin{aligned}
& \mathcal{H}_{\text{int}}(z, \bar{z})\mathcal{H}_{\text{int}}(w, \bar{w}) \\
& \sim \frac{1}{|z-w|^2} \left((16g^2 + t^2 + y^2 + w^2) \sum_{a,b} G_{ab}^R G_{ab}^L + (16gt + 2t^2 + 2y^2 - 2w^2) \sum_a T_a^R T_a^L \right. \\
& \left. + (16gy + 4ty + 2w^2) \sum_a V_a^R V_a^L + (16gw - 4tw + 4yw) \frac{1}{\sqrt{2}} \sum_a (T_a^R V_a^L + V_a^R T_a^L) \right), \tag{B.21}
\end{aligned}$$

which gives rise to the RG equations:

$$\begin{aligned}
\frac{dg}{dl} &= 16g^2 + t^2 + y^2 + w^2, \\
\frac{dt}{dl} &= 16gt + 2t^2 + 2y^2 - 2w^2, \\
\frac{dy}{dl} &= 16gy + 4ty + 2w^2, \\
\frac{dw}{dl} &= 16gw - 4tw + 4yw. \tag{B.22}
\end{aligned}$$

The RG equations can be solved analytically on $SO(7)$ symmetric fixed planes. On the $SO(7)_A$ symmetric fixed plane, namely $t = 2g, w = 0$, the RG equation have only two independent variables, which can be chosen as y and $x = g + \frac{t}{2}$. The RG equations are reduced to

$$\frac{dy}{dx} = \frac{6xy}{5x^2 + y^2}, \tag{B.23}$$

whose solution is $(x^2 - y^2)^3 + Cy^5 = 0, \forall C \in \mathbb{R}$. This set of curves have asymptotic lines $y = x, y = -x$ and $y = 0$, corresponding to the $SO(8)$ GN fixed flow $t = y = 2g, w = 0$, the $SO(8)_A$ GN fixed flow $t = -y = 2g, w = 0$, and the $SO(7)_A$ GN fixed flow $t = 2g, y = w = 0$, respectively. The plot of these solution curves are shown in figure 5, which looks the same as figure 2 in the main text. According to the triality, the RG flows on the other two $SO(7)$ symmetric fixed planes are the same.

The RG equations can be also investigated in terms of g, t_A, t_B, t_M by employing the relation between T'_a, V'_a, T''_a, V''_a and T_a, V_a . The OPE reads

$$\begin{aligned}
& \mathcal{H}_{\text{int}}(z, \bar{z})\mathcal{H}_{\text{int}}(w, \bar{w}) \\
& \sim \frac{1}{|z-w|^2} \left(\left(16g^2 + t_A^2 + t_B^2 + t_M^2 + \frac{1}{2}t_A t_B + \frac{1}{2}t_B t_M + \frac{1}{2}t_M t_A \right) \sum_{a,b} G_{ab}^R G_{ab}^L \right. \\
& + (16gt_A + 2t_A^2 + 4t_B t_M) \sum_a T_a^R T_a^L + (16gt_B + 2t_B^2 + 4t_M t_A) \sum_a T_a'^R T_a'^L \\
& \left. + (16gt_M + 2t_M^2 + 4t_A t_B) \sum_a T_a''^R T_a''^L \right),
\end{aligned}$$

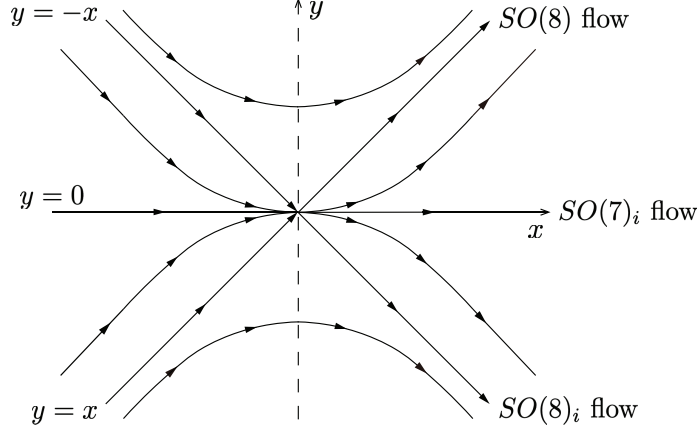


Figure 5. RG flow on $SO(7)$ symmetric fixed planes.

which gives rise to the RG equations in the main text:

$$\begin{aligned}\frac{dg}{dl} &= 16g^2 + \sum_i t_i^2 + \frac{1}{4} \sum_{i \neq j} t_i t_j, \\ \frac{dt_i}{dl} &= 16gt_i + 2t_i^2 + 4 \frac{t_A t_B t_M}{t_i},\end{aligned}\tag{B.24}$$

where i, j, k range in A, B, M . The RG flows on $SO(7)$ fixed planes are the same as figure 5.

Except for fixed flows and fixed planes, the RG equations (B.24) also have fixed bodies, i.e. three dimensional bodies in the parameter space in which RG flows keep inside evolution. From (B.24), it is not hard to derive that

$$\frac{d}{dl} \left(\sum_i t_i \right) = 16g \left(\sum_i t_i \right) + 2 \left(\sum_i t_i \right)^2\tag{B.25}$$

$$\frac{d}{dl} (t_i - t_j) = \left(16g + 2t_i + 2t_j - 4 \sum_k \epsilon_{ijk} t_k \right) (t_i - t_j).\tag{B.26}$$

Therefore, both $\sum_i t_i = 0$ and $t_i = t_j$ are solutions to the RG equations (B.24), and hence define four fixed bodies in the parameter space: $t_A + t_B + t_M = 0$, $t_A = t_B$, $t_B = t_M$, and $t_M = t_A$. The intersections of these fixed bodies will give rise to some fixed planes.

C Bosonization of the interaction on $SO(7)$ symmetric fixed planes

For simplicity, we use the interaction Hamiltonian density on $SO(7)_M$ symmetric fixed plane which is directly written in terms of Majorana operators defined in (A.7). Hamiltonian densities on the other two $SO(7)$ symmetric fixed planes can be similarly solved via triality relation.

$$\mathcal{H}_M = g \sum_{1 \leq m, n \leq 7} (i\chi_m^R \chi_n^R)(i\chi_m^L \chi_n^L) + 3(2g - t_M) \sum_{1 \leq m \leq 7} (i\chi_0^R \chi_m^R)(i\chi_0^L \chi_m^L).\tag{C.1}$$

It can be rearranged into a Gross-Neveu form (up to a constant)

$$\mathcal{H}_M = -g \left(\sum_{1 \leq m \leq 7} i\chi_m^R \chi_m^L + \left(3 - \frac{3t_M}{2g} \right) i\chi_0^R \chi_0^L \right)^2. \quad (\text{C.2})$$

Therefore, when $t_M = 2g$, i.e. on the $SO(7)_M$ GN fixed flow, χ_0 is decoupled in the interaction and becomes massless, corresponding to an Ising phase transition with central charge $c = \frac{1}{2}$.

According to a standard bosonization dictionary

$$i\chi_4^R \chi_4^L + i\chi_0^R \chi_0^L \sim \frac{1}{\pi a} \cos \sqrt{4\pi} \phi_{\frac{3}{2}}, \quad i\chi_4^R \chi_4^L - i\chi_0^R \chi_0^L \sim \frac{1}{\pi a} \cos \sqrt{4\pi} \theta_{\frac{3}{2}}, \quad (\text{C.3})$$

the Hamiltonian density above can be bosonized as

$$\mathcal{H}_M = - \frac{g}{(\pi a)^2} \left(\sum_{\sigma \neq \frac{3}{2}} \cos \sqrt{4\pi} \phi_\sigma + \left(2 - \frac{3t_M}{4g} \right) \cos \sqrt{4\pi} \phi_{\frac{3}{2}} + \left(-1 + \frac{3t_M}{4g} \right) \cos \sqrt{4\pi} \theta_{\frac{3}{2}} \right)^2. \quad (\text{C.4})$$

where in the second equality the derivative terms $-\frac{2}{\pi}(\partial_\mu \phi)^2 = (\cos \sqrt{4\pi} \phi)^2$ are dropped. Consider $g > 0$ case where the interactions are always relevant. For all t_M , the local minima of this bosonized Hamiltonian have ϕ_σ , $\sigma \neq \frac{3}{2}$ pinned. For $\sigma = \frac{3}{2}$, the local minima have $\phi_{\frac{3}{2}}$ pinned when $t_M < 2g$, and $\theta_{\frac{3}{2}}$ pinned when $t_M > 2g$. This also suggests that $t_M = 2g$ is an Ising transition point with central charge $c = \frac{1}{2}$. When $t_M = \frac{4}{3}g$ or $\frac{8}{3}g$, the bosonized Hamiltonian has $SO(8)$ symmetries which is consistent with $SO(8)$ and $SO(8)_M$ fixed flows obtained from RG equations, respectively.

D RG for the lattice model

We numerically integrate the RG equations on the lattice model phase diagram $P_{\text{Lat}} : t_A + t_B = 0$, $t_M = -4g$. Since $u(v) = 0$ on the $v(u)$ -axis, lattice model couplings u and v are related to continuum model parameters as $u = C_0(t_A - kg)$ and $v = C_0(t_B - kg)$. $C_0 > 0$ is an undetermined constant related to the details of coarse-graining and cutoff, which is irrelevant to our discussions. The initial values for RG equations are chosen as

$$g(0) = r_0 \cos \theta, \quad t_A(0) = -4r_0 \sin \theta, \quad t_B(0) = 4r_0 \sin \theta, \quad t_M(0) = -4r_0 \cos \theta, \quad (\text{D.1})$$

where θ varies from 0 to 2π and $r_0 > 0$. Thus, the initial values of u and v are

$$u(0) = R_0 \cos \left(\theta + \frac{\pi}{4} \right), \quad v(0) = R_0 \sin \left(\theta + \frac{\pi}{4} \right), \quad (\text{D.2})$$

where $R_0 = 2\sqrt{2}C_0r_0 > 0$. Therefore, $u = v > 0$ axis, positive v -axis, negative u -axis, $u = v < 0$ axis, negative v -axis and positive u -axis are corresponding to $\theta = 0, \frac{1}{4}\pi, \frac{3}{4}\pi, \pi, \frac{5}{4}\pi$ and $\frac{7}{4}\pi$. In numerics we find a critical $\theta_c = (0.705 \pm 0.002)\pi$ for all $r_0 > 0$, such that when $0 < \theta < \theta_c$, the RG flows are controlled by the $SO(8)_B$ GN fixed flow, suggesting

the gapped $SO(8)_B$ GN phase; when $\theta_c < \theta < \pi$ and $\pi < \theta < 2\pi - \theta_c$, the RG flows are controlled by the $SO(8)$ GN fixed flow, suggesting the $SO(8)$ GN phase; and when $2\pi - \theta_c < \theta < 2\pi$, the RG flows are controlled by the $SO(8)_A$ GN fixed point, suggesting the $SO(8)_A$ GN phase. In numerics, we locate θ_c by the sign change of t_A and t_M around it which suggests a phase transition controlled by the $SO(7)_B$ GN fixed flow with central charge $c = \frac{1}{2}$. The situation of $\theta = 2\pi - \theta_c$ is similar, where the phase transition is controlled by the $SO(7)_A$ GN fixed flow. When $\theta = 0$ and $\theta = \pi$, the RG flows are controlled by the G_2 TCI and the $SO(7)_M$ GN fixed flows, suggesting phase transitions with central charges $c = \frac{6}{5}$ and $c = \frac{1}{2}$, respectively. Note that

$$\frac{v(0)}{u(0)} = \tan\left(\theta_c + \frac{\pi}{4}\right) \approx -\frac{1}{7}, \quad (\text{D.3})$$

with a deviation in θ_c (with respect to 2π) less than 0.2%. This suggests that the equation of the $SO(7)_B$ phase transition line is consistent with the predicted location $u = -7v$ based on a mean-field analysis. The acceptably small deviation of 0.2% arises from the perturbative nature of the one-loop RG method. By a similar argument, the $SO(7)_A$ transition line is $v \approx -7u$.